



# Mass exchange in close binaries: theories vs observations

D.V. Bisikalo and D.A. Kononov

Institute of Astronomy of the Russian Academy of Sciences, 48 Pyatnitskaya street, 119017, Moscow, Russia, e-mail: bisikalo@inasan.ru

**Abstract.** In this report we present the review of 3D gas dynamic models used for the description of the mass exchange in close binaries. Main features of the flow structure in steady-state close binaries are summarized. The special attention is paid to physics of accretion disks in binary systems and particularly to waves in the disks. The gas-dynamical simulations combined with the Doppler tomograms have made it possible to identify basic features of the flow structure. Comparisons between the synthetic tomograms and observations enable identification of the flow regions responsible for zones of enhanced emission in the Doppler maps, thus determining the gas-flow pattern in the system. Our analysis indicates that the main contributions to the luminosity in the tomogram are made by the arms of the spiral tidal shock, the shock formed due to interaction between the circum-disk halo and the stream from the inner Lagrange point  $L_1$  ("hot line"), and the bow shock caused by the motion of the accretor and the disk in the gas of the circum-binary envelope.

**Key words.** Stars: binaries – Stars: cataclysmic variables – Stars: accretion disks – Stars: Doppler tomography – Stars: 3D gas dynamic simulations

## 1. Introduction

Stars named cataclysmic variables (CVs) are close binary systems where the mass transfer from one component to another exists. In the middle of the XX<sup>th</sup> century it became evident that the various observational phenomena demonstrated by cataclysmic variables are due to the accretion of matter onto a white dwarf from a low mass donor star filling its Roche lobe. The behavior of CVs is characterized by two states of activity: quiescence and outbursts. Systems which are usually faint enough while quiescent can increase their brightness by as much as  $4^m$ - $5^m$  during outburst, traditionally explained by a temporary increase in the

rate of accretion onto the primary component (white dwarf) of the binary.

Today it is recognized that life of a cataclysmic variable is mostly ruled by the mass transfer and accretion character. So the detailed study of gas dynamics of CVs during both states is needed to understand physical processes running in them and their further evolution.

Observationally information about the basic features of the flow pattern can be obtained using Doppler-tomography techniques (Marsh & Horne 1988). This method transforms the orbital variability of emission-line intensities into luminosity maps in the two-dimensional velocity space ( $V_x, V_y$ ). In some cases, resulting Doppler maps can be inter-

---

Send offprint requests to: D. Bisikalo

preted more straightforwardly than the original spectrograms; in addition, a tomogram can indicate (or at least give some idea of) some characteristic features of the matter-flow structure. In particular, lines with double-humped profiles, corresponding to circular motions (e.g., in an accretion disk), are transformed into a blurred ring in the Doppler map. In other words, the components of a binary can be resolved in the velocity space, while they cannot be spatially resolved by direct observations; therefore, the Doppler-tomography technique is a powerful tool for investigating binaries. Unfortunately, the problem of reconstructing the spatial distributions of emission-line intensities from a Doppler map does not have a general solution, since points that are very distant from one another can have the same velocities and contribute to the same location in the Doppler map. Thus, the transform  $I(V_x, V_y) \rightarrow I(x, y)$  is not possible unless some *a priori* assumptions about the velocity-field structure are made.

Gas-dynamical computations can be used to find a solution of this problem. The computed fields of the density,  $\rho(x, y)$ , and temperature,  $T(x, y)$ , can be used to obtain the emission-intensity distribution. Based on the computed velocity  $V(x, y)$ , this distribution can easily be transformed into a synthetic Doppler map. Comparisons of observed and synthetic tomograms enable identification of the flow regions responsible for zones of enhanced emission in Doppler maps, thus revealing features in the flow structure characteristic of a system under study.

To study the flow pattern in CVs from both theoretical and observational points of view we chose the well-known system SS Cyg. The components of the semi-detached SS Cyg binary are an  $K(4-5)V$  (Smith & Dhillon 1998) red dwarf with a mass of  $\sim 0.56 M_\odot$  and a radius of  $\sim 0.68 R_\odot$  and a white dwarf with a mass of  $\sim 0.97 M_\odot$  and a radius of  $\sim 0.007 R_\odot$  (Giovannelli et al. 1983). The red dwarf loses matter at a rate of  $10^{-9} - 10^{-8} M_\odot$  per year. The component separation is  $2.05 R_\odot$ , and the orbital period of the system is 6.6 hr.

We have carried out spectral-line observations of SS Cyg in August and December

2006 using the 2-m telescope at Terskol Peak. The observations were carried out during both states. In parallel, we carried out three-dimensional gas-dynamical simulations of the SS Cyg system. For the quiescent state we have constructed a synthetic Doppler map based on the simulation result and compared it with observational Doppler maps, in order to interpret the observations and derive some information about the flows of matter in the system. For the active state we obtained a series of spectra and on the results of their analysis we propose a model describing the matter flow structure during outburst.

The detailed studies of SS Cyg for the particular states are described in papers Bisikalo et al. (2008) and Kononov et al. (2008). Here we summarize obtained results to show on example of a real system that the complex study based on gas dynamic simulations and the Doppler tomography can reveal the flow pattern in a close binary system and bring understanding of physical processes running in the system during both states.

## 2. Three-dimensional gas dynamic simulations and synthetic Doppler map

We performed three-dimensional numerical studies of the matter-flow structure in the quiescent SS Cyg system using the model of Bisikalo et al. (2008), carrying out our computations until the flow settled down to a steady-state regime. The numerical code employed was based on a Godunov-type finite difference scheme with a high order of accuracy. We used a geometrically adaptive mesh to enhance the resolution of the vertical structure of the accretion disk and describe the immediate neighborhood of the accretor's boundary. We included radiative heating and cooling in the same manner as in Bisikalo et al. (2003). The calculations were performed in a non-inertial reference system rotating together with the binary system. The morphology of the gas flows in the binary system is shown in Fig. 1. The upper diagram in Fig. 1 shows the density distribution and the velocity vectors in the

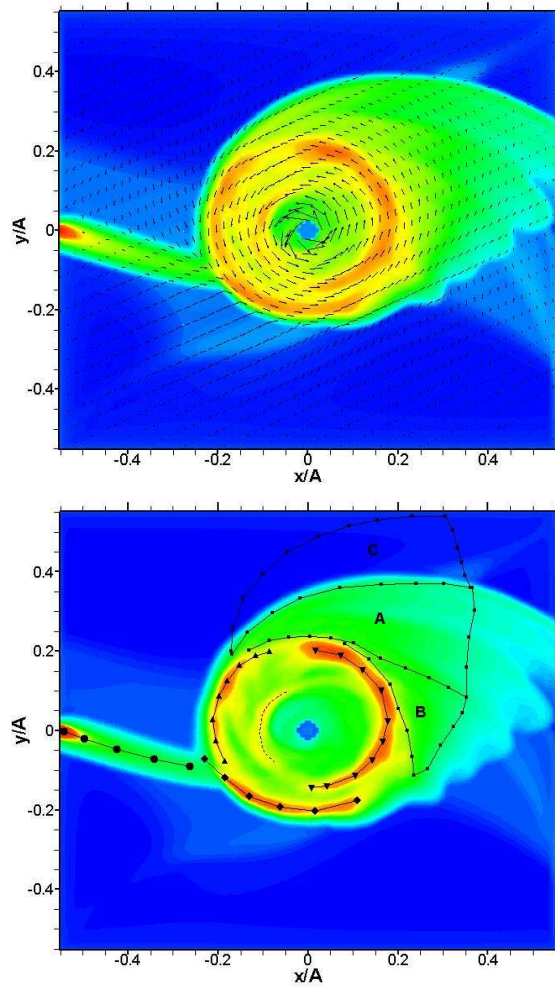


**Fig. 1.** Results of three-dimensional gas dynamic simulations. The top panel shows the distribution of the logarithm of the matter density and velocity vectors in the equatorial plane of the system, and the bottom panel the distribution of the logarithm of the intensity of recombination emission. The markers in the bottom diagram correspond to the principal features of the flow – the stream from  $L_1$  point (solid curve with circles), the "hot line" (solid curve with diamonds), the two arms of the spiral tidal shock (solid curves with triangles; the arms can be distinguished by the vertex direction of the triangles), and the precession spiral wave (dashed curve). Three regions of the circum-binary envelope around the bow shock are also shown in the bottom diagram (solid black curves with small squares, labeled as A, B, C).

equatorial plane of the system (the  $XY$  plane). The density values are plotted on a logarithmic scale, as fractions of the matter density at the inner Lagrangian point,  $\rho_0$  (we assumed in our computations that the matter density at  $L_1$  is  $3.1 \times 10^{-8} \text{ g cm}^{-3}$ , which corresponds to a mass exchange rate between compo-

nents of the system of  $8 \times 10^{-9} M_{\odot}/\text{year}$ ). An analysis of these results and of our previous studies (Boyarchuk et al. 2002; Bisikalo et al. 2003; Bisikalo & Matsuda 2007; Fridman & Bisikalo 2009), indicates that gas dynamics of the matter flow in a semi-detached binary system is determined by

the presence of the matter stream from  $L_1$ , the quasi-elliptical accretion disk, the circum-disk halo, and the circum-binary envelope. The classification of the basic features of the flow pattern introduced in Boyarchuk et al. (2002) is based on their physical properties: (a) if the flow is not governed by the gravitational field of the accretor, the gas forms a circum-binary envelope that fills the space between and around the components; (b) if the gas revolves about the accretor and later mixes with matter in the stream, this gas does not belong to the disk, and instead forms a circum-disk halo; (c) the accretion disk is formed from matter of the stream that no longer interacts with the stream once its motion is dominated by the gravitational field of the accretor. The interaction between the gas of the circum-disk halo and the stream results in the formation of a shock, the so-called "hot line". The tidal influence of the donor gives rise to a two-armed spiral shock. The motion of the accretor and the disk in the gas of the circum-binary envelope leads to the formation of the bow shock. An additional element of the flow structure – the precessional spiral wave forms in the inner region of the accretion disk, which is free of gas-dynamical perturbations, such as tidal waves or the "hot line" (Bisikalo et al. 2003, 2004, 2005). In this region, forces related to the gas-pressure gradient become small compared with gravitation, that specifies the flow structure in this part of the disk. The flowlines formed in the disk under action of these forces are elliptical, with the accreting star at one focus. The asphericity of the gravitation field of a binary star results in precession of each flowline. The precessional period of each flowline is fairly large, and decreases with increasing of the semi-major axis. Since the flowlines in a gaseous disk cannot intersect, they interact, forming a spiral structure – the precessional spiral density wave.

The morphology of gaseous flows in the considered binary system can be evaluated from 1 (upper panel). In this figure the distribution of the density over the equatorial plane and velocity vectors are presented. The bottom panel in Fig. 1 represents the distribution of the logarithm of the intensity of the re-

combination emission (in arbitrary units) in the equatorial plane of the system. To determine the intensity, we used densities and temperatures based on the gas dynamic calculations, and adopted the recombination coefficients for the Menzels case B from Storey & Hummer (1995). The markers correspond to the principal features of the flow. The matter stream from  $L_1$  point is shown as a solid curve with circles, the "hot line" as a solid curve with diamonds, two arms of the spiral tidal shock as solid curves with triangles (the arms can be distinguished by the vertex direction of the triangles). In the bottom diagram, three regions of the circum-binary envelope around the bow shock are also shown (black solid curves with small squares, labeled A, B, C). It is important to note, that solution for system with moderate magnetic field has the same principal features (Zhilkin & Bisikalo 2009a,b): (i) the magnetized accretion disk forms in the system; (ii) all previously discovered waves are still exist in the disk: the "hot line", two arms of the tidal shock, spiral precessional wave, and bow shock.

Using the results of the simulations we constructed a synthetic Doppler map of SS Cyg shown in the upper panel of Fig. 2. Markers corresponding to those in the bottom diagram in Fig. 1 are placed in the Doppler map. Note that the upper panel of Fig. 2 presents the instantaneous intensity distribution obtained for a certain time, and corresponds to the velocity field determined only for that time. Therefore, features that exhibit proper motions in the rotating coordinate system will, together with others, be visible in the synthetic Doppler map, but will not be represented in an observational tomogram. In particular, the precessional spiral wave shown in the synthetic Doppler map by the white dashed curve should not be present in the observational tomograms.

### 3. Observations and observed Doppler maps

We carried out our observations during 5 nights; one night during quiescent state and four nights for two outbursts in August and December 2006. We observed with

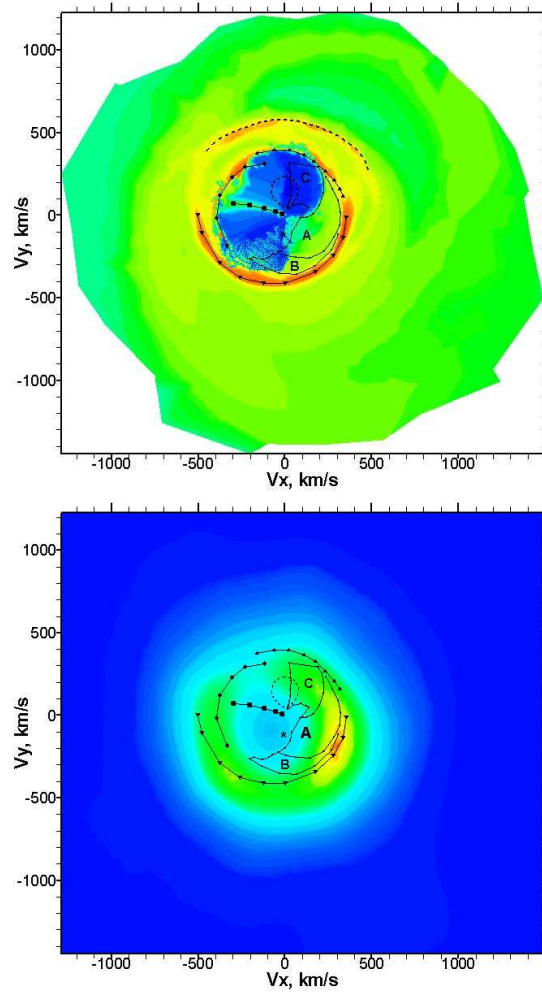


**Fig. 2.** Upper panel: Synthetic Doppler map of the SS Cyg system. Lower panel: Observational Doppler tomogram obtained in the  $H_\gamma$  line. The markers in the both maps correspond to those in the bottom diagram of Fig. 1.

the two-meter telescope Zeiss-2000 of the Terskol observatory (Terskol, Russia) using the Cassegrain spectrograph working in a classical mode. The star was observed in two wavelength ranges of  $3800 - 5200 \text{ \AA}$  and  $6000 - 7000 \text{ \AA}$  with a mean inverse dispersion of  $1.16 \text{ \AA/pixel}$ . The exposure time was  $\tau = 15 \text{ min}$ . We referenced the spectra to the phase of the binary using the ephemeris of North et al. (2002),

$$T_0 = 2450622.5483(2)(HJD),$$

where  $T_0$  is the epoch when the radial velocity passes through zero from negative to positive values.

After the data processing we obtained for the quiescent state in groups of 19 profiles of the  $H_\beta$  and  $H_\gamma$  lines and for outbursts 20 profiles of the  $H_\alpha$  line (August outburst) and for the  $H_\beta$  and  $H_\gamma$ : in groups of 2 profiles on December 8; in groups of 3 profiles on December 10 and in groups of 13 profiles on December 13 2006.

Observational Doppler maps were constructed using the spectra of  $H_\alpha$  (active state),  $H_\beta$  and  $H_\gamma$  (quiescent state) line profiles. To construct the maps we used a restoration code developed in the INASAN based on the solving of the linear system

$$\mathbf{D} = H \times \mathbf{I}(V_x, V_y),$$

where  $\mathbf{D}$  and  $\mathbf{I}(V_x, V_y)$  are vectors of the dirty and restored images respectively and  $H$  is a matrix representing the PSF. We obtained the regularized solution, using the Maximum Entropy regularization. The constructed Doppler tomogram in the  $H_\gamma$  line is shown in the lower panel of Fig. 2.

#### 4. Comparison of the synthetic and observational Doppler map in quiescence

To make comparisons between the synthetic and observational tomograms more convenient, we present the observational tomogram with the same markers as in the synthetic map. We conclude from such comparisons that the spiral tidal shock and the regions of the circum-binary envelope located near the bow-shock make the main contributions to the luminosity in the tomogram. The markers denoting the tidal-shock arm more distant from the donor clearly fall on the bright region in the lower quadrants of the tomogram. The region of enhanced brightness that can be identified with the tidal shock arm closer to the donor corresponds here to somewhat lower velocities than in the synthetic map. This may be due to various physical factors (e.g., the size of the observed accretion disk slightly exceeds the size of the simulated disk), or the fact that the observational tomogram is a superposition of the contributions from this arm of the tidal shock and the region behind the bow-shock. The envelope regions near the bow-shock (zones A, B, C) are characterized by low velocities and significant brightnesses. Therefore, due to the insufficient resolution of the available line profiles, the brightness peak in the tomogram is shifted toward lower velocities.

The relatively poor resolution of the original spectra prevents the identification of low-

contrast features that are clearly visible in the synthetic map. In particular, the matter stream from the  $L_1$  point is virtually indistinguishable in the tomograms. The "hot line" region can be identified in the observational tomogram, but not as a specific feature. The presence of a brightening near the "hot line" (which is pronounced in the synthetic map) modifies the brightness gradient at this place in the observational tomogram, suggesting that the "hot line" is, indeed, present in the flow.

The clear asymmetry of the inner parts of the observational tomograms is among their most pronounced features. The similar asymmetry in the synthetic map is formed by the emission of matter of the circum-binary envelope in the region behind the bow-shock (Figs. 1, 2, zone A). A considerable contribution to the observational tomograms is also made by zones B and C, next to zone A. Their contribution is not as pronounced in the synthetic map, but differences of the real from the computed system could be large enough to explain these difference (for example, the position of the bow-shock varies with time, even in the quasi-stationary computational run (Syrov, Kaigorodov & Bisikalo 2007)).

#### 5. Analysis of observations obtained during outburst

The line profiles of SS Cyg are rather complex during outburst. In Figure 3 changes of the  $H_\gamma$  profile structure during the outburst progress is shown. First of all we should note that an absorption component appears at the beginning of outburst. During the decline of the light curve, the depth of the absorption component diminishes and in the quiescent state this component disappears completely. The emission component changes under a complex law and has a minimum on December 10 right after the maximum of the brightness.

Various parts of the flow with different velocities and velocity dispersions contribute to a line profile formation. The wavelength ranges emitted by different flows overlap, making the problem of subdividing the profile into components ambiguous: the line profile can be subdivided in several ways. In this process, advan-

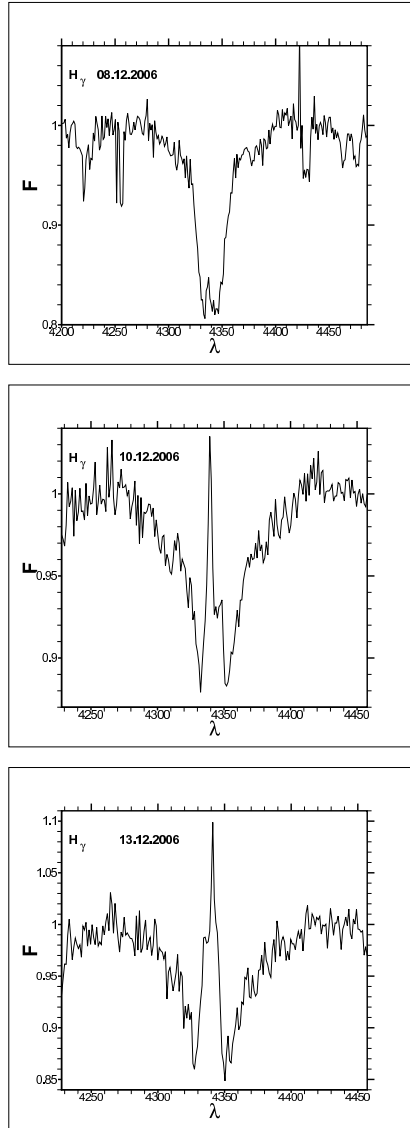


**Fig. 3.** Long-term evolution of the  $H_\gamma$  line profile during outburst.

tages of one subdivision compared to others can be identified only using additional assumptions concerning the parameters of the flows that formed the line profile. Nevertheless, we can attempt to use the line shape and dynamics of its variations to tentatively subdivide the

line into its main components and compare the results to elements of gas dynamical pattern in the system.

In this way, we can subdivide the  $H_\alpha$ ,  $H_\beta$  and  $H_\gamma$  line profiles into three main components, namely a broad absorption component and two emission components: a broad pedestal and a narrow peak. Note that we did not observe any absorption component in the  $H_\alpha$  line during outburst or in the  $H_\beta$  or  $H_\gamma$  lines in quiescence.

Based on our observations, we suggest the following scenario for the development of an outburst of SS Cyg. At some time, an instability develops in the disk, leading to a considerable increase of the efficiency of the angular-momentum transport and an increase in the accretion rate. The growing intensity of the radiation from the white dwarf inevitably results in heating of the nearest parts of the accretion disk, and hence to an increase of the thickness of inner parts of the disk. As a result, a toroidal shell forms around the accretor (region C in Fig. 4), obscuring the accretor from the observer and leading to the appearance of absorption components in the  $H_\beta$  and  $H_\gamma$  lines. The  $H_\gamma$  absorption line is substantially non-Gaussian, and can be subdivided into two components: a narrow one due to the intrinsic keplerian motions in the toroidal shell, and a broad one due to the Stark effect. Our analysis of the narrow component enables us to identify the region where the toroidal shell is formed. It was shown that the broadening of the narrow absorption component and the corresponding velocity dispersion suggested that the toroidal shell forms in the immediate vicinity of the accretor. Considering the broad component, we see that the contribution of the wings to the resulting line half-width is comparatively low:  $\sim 10 - 15\%$ . The slope of the broadened wings can be used to estimate the density in the toroidal shell. If the broadening is due exclusively to the Stark effect, the density of particles in the inner parts of the toroidal shell should be  $10^{16} - 10^{17} \text{ cm}^{-3}$ .

The gas between the toroidal shell and the accretor experiences strong heating that leads to its expansion. However, the expansion cannot be isotropic, since it is restricted in the

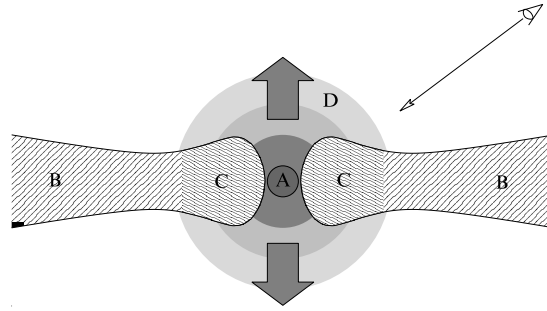


**Fig. 4.** Structure of the matter flows in the region near the accretor. The plane of the disks rotation is perpendicular to the plane of the figure. The letters denote the accretor (A), accretion disk (B), toroidal shell (C), and spherical shell (D). The arrow with an open end represents the observers line of sight, and the big gray arrows show the direction of motion of matter in the spherical shell.

equatorial plane by the accretor surface and the inner surface of the toroidal shell, whereas expansion perpendicular to the disks surface is impeded only by the accretors gravitational field. The expansion velocity of the heated gas will probably be comparable to the local sound speed, which is insufficient to form a collimated jet. The expanding gas can have a low angular velocity, and is prevented from falling on the star primarily by the gas-pressure gradient rather than by the centrifugal force. This enables the gas to leave the toroidal shell and form an expanding spherical shell around the accretor (region D in Fig. 4). The increased size of this shell can explain the stronger emission during the development of the outburst. It is obvious that the mentioned above pedestal corresponds to the radiation from the spherical shell: its orbital shifts agree with the accretors projected orbital velocity. In turn, the broadening of the pedestal in the course of the outburst development can be explained by the transfer of angular momentum to matter in the spherical shell from the toroidal shell, accompanied by an increase in the angular velocity in the spherical shell.

The outer parts of the accretion disk also should contribute to the line pedestal. The contribution from the spherical shell is still low at the beginning, and even at the maximum, of the outburst, so that the line pedestal is mainly formed by outer parts of the residual accretion disk at these stages. An analysis of the integrated emission-line luminosity shows that

the luminosity is approximately a factor of ten lower at the outburst maximum than in quiescence, suggesting that the contribution to the binarys luminosity from the outer parts of the residual accretion disk is small.

During outburst, the flux increases not only in the visible, but also in the ultraviolet and soft X-ray Wheatley, Mauche, & Mattei (2003). The accretion disk is optically thin at such wavelengths, permitting the radiation to freely reach the surface of the donor, heating it and leading to a growth in the donor emission. Naturally, the strongest heating occurs at the parts of the star that are closest to the inner Lagrange point, whose light forms the peak of the second emission component identified above. Clearly, the bright spot in the  $H_\alpha$  tomogram is also due to heating of the donor.

In general, a comparison of the  $H_\alpha$  tomogram (Kononov et al. 2008) and those obtained for quiescence (Bisikalo et al. 2008) reveals considerable changes in the observed structure. The much smaller number of tomogram details during outburst and their fuzziness are striking. In fact, we are not even able to estimate the outer size of the accretion disk from the tomogram because the inner limit of the corresponding ring is missing. We can suggest several explanations for this. First, as noted above, the luminosity of the residual accretion disk is low due to the re-distribution of matter during outburst, with a substantial portion being accumulated in the optically thick toroidal shell. The inner re-



gion of the tomogram "ring" can be filled due to radiation from low-velocity matter in the spherical shell. In addition, the image could be smeared due to the presence of non-stationary flows in the binary, which are visible only at certain phases. Indirect confirmation of the presence of such flows is provided by the features in the radial-velocity curves observed at phases  $\sim 0.25$  and  $\sim 0.75$  and the slight asymmetry of the tomogram (Kononov et al. 2008). As was demonstrated in Bisikalo et al. (2008), such asymmetry could be due to radiation from matter located immediately in front of the bow shock formed during the orbital motion of the accretion disk. It was shown in Sytov, Kaigorodov & Bisikalo (2007) that interactions between the accretion disk and bow shock can give rise to quasi-periodic outflows at some phases. The conclusions in the above cited papers were drawn solely for quiescence, but the flows of matter that are ejected by the binary and take away angular momentum should be higher during outburst than in quiescence. The observed tomogram asymmetry may provide indirect evidence for the presence of a large amount of heated matter in front of the bow shock.

When the star emerges from outburst, the thickness of the toroidal shell should decrease, leading to a decrease in the absorption component's depth. In turn, the decreased flux from the star should lead to a contraction of the spherical shell: matter is ejected into this shell due to heating of gas by radiation. This leads to a decrease in the emission peak to levels comparable to the emission from the residual accretion disk. The emission in the spectra obtained on December 13 (see Fig/ 3) is probably mainly due to the disk.

## 6. Conclusions

We have compared observational and synthetic tomograms in order to identify the main features of the flow pattern in the quiescent SS Cyg system. The observational tomograms were based on a series of spectra obtained in the  $H_\beta$  and  $H_\gamma$  lines in August 2006 using the two meter telescope of the observatory at the

Terskol Peak. The synthetic map was based on three-dimensional gas dynamic calculations.

The gas dynamic simulations combined with the Doppler tomograms have made it possible to identify certain basic features of the flow pattern in the synthetic Doppler map without solving an ill posed inverse problem. Our analysis indicates that the main contributions to the luminosity in the tomogram during the quiescent state are made by the arms of the spiral tidal shock, the shock due to the interaction of the circum-disk halo with the matter stream from  $L_1$  point ("hot line"), and the region of the circum-binary envelope near the bow-shock. The contribution of this last region results in appreciable asymmetry of the tomograms.

To study the structure of matter flows during the active state of SS Cyg, we have performed spectroscopy during two outbursts, in August and December 2006. In August, we acquired spectra in the  $H_\alpha$  line and in December, in the  $H_\beta$  and  $H_\gamma$  lines. The spectra from our December observing run were taken on several nights, making it possible to detect and analyze spectral line profile variations with the development of the outburst. A series of 13 spectra taken on December 1314, 2006 reveal orbital variations of the line profiles. All the  $H_\alpha$  profiles for the August outburst were taken during a single night. The absence of observed absorption in the line made it possible to construct a Doppler map and use it to analyze the flow pattern of the system.

Our analysis of the spectra and Doppler tomogram demonstrates that the lines are formed in at least five flow regions in the system: in the outer parts of the residual accretion disk; at the surface of the donor around the inner Lagrange point  $L_1$  that are heated by the extra radiation from the accretor; in a toroidal shell, which is a thickening at the inner edge of the accretion disk; in a spherical shell around the accretor; and in the region around the bow-shock.

## 7. DISCUSSION

**G.E. Romero** How the disk waves might affect the production and stability of jets?

**D. Bisikalo** Shock waves are located at the outer parts of the accretion disk, so they can not influence on the jet collimation mechanism. On the other hand the presence of the shocks stimulate the angular momentum transfer and can lead to the significant increasing of the accretion rate, and as a consequence to the increasing of the jet intensity.

**A. Zdziarski** Can you obtain the fraction of matter not falling onto the accretor from some first principles?

**D. Bisikalo** The fraction of accreting matter depends on the angular momentum transfer mechanism. If you assume the presence of some specific mechanism you can get a fraction of accreting matter. For typical set of mechanisms in accretion disks in binaries (tidal influence, shocks, and turbulent viscosity) included in our numerical model the fraction of accreting matter is not higher than 20-30%, in case if you include into consideration the magnetic field (Zhilkin & Bisikalo 2009a,b) the accretion rate can be as much as 50%.

**P. Selvelli** Could you give an estimate of the relative importance of the three mentioned shock waves at different wavelengths and different system inclination angles?

**D. Bisikalo** Considered shocks are located at the outer edge of the accretion disk so their visibility is more less the same at specific inclination angles, while the visibility is strongly depend on the phase angle. The strengths of shocks are different (the most intensive is the hot line, bow shock is moderate, and tidal shocks are weak), so they will give their main input into different wavelengths.

**A. Zdziarski** What is the fate of matter in the circum-binary envelope?

**D. Bisikalo** The matter forming the circum-binary envelope has enough energy to escape the system, so at distances above

10–15 system separations we see in the model the formation of diffuse excretion disk (Sytov, Kaigorodov & Bisikalo 2007).

*Acknowledgements.* The work was supported by the Russian Foundation for Basic Research (projects no. 08-02-00371, 08-02-00928, 09-02-00064, 09-02-00993), the Scientific Schools Program (grant no. NSh- 4354.2008.2), and the basic research program "Origin, structure and evolution of objects in the Universe" of the RAS.

## References

- Bisikalo, D. V., et al. 2003, *Ast. Rep.*, 47(10), 809  
 Bisikalo, D. V., et al. 2004, *Ast. Rep.*, 48, 588  
 Bisikalo, D. V., et al. 2005, *Ast. Rep.*, 49, 701  
 Bisikalo, D. V. & Matsuda T. 2007, *Proceedings of IAU Symposium 240*, Cambridge: Cambridge University Press, 356.  
 Bisikalo, D. V., et al. 2008, *Ast. Rep.*, 52(4), 318  
 Boyarchuk, A. A., et al., 2002, "Mass Transfer in Close Binary Stars", Taylor and Frances, London, 365 p.  
 Fridman, A. M. & Bisikalo, D. V. 2008, *Physics - Uspekhi*, 51 (6), 551  
 Giovannelli, F. et al. 1983, *Acta Astron.*, 33, 319  
 Kononov, D. A., et al. 2008, *Ast. Rep.*, 52(10), 835  
 Marsh, T. R., & Horne K., 1988, *MNRAS*, 235, 269  
 North, R. C. et al., 2002, *MNRAS*, 337, 1215  
 Smith, R. C., & Dhillon, V. S., 1998, *MNRAS*, 301, 767  
 Storey, P. J. & Hummer, D. G., 1995, *MNRAS*, 272, 41  
 Sytov, A. Yu., Kaigorodov P. V., & Bisikalo D. V., 2007, *Ast. Rep.*, 47, 836  
 Zhilkin, A. G., & Bisikalo, D. V., 2009 a, *ASP Conference Series*, 406, 118  
 Zhilkin, A. G., & Bisikalo, D. V., 2009 b, *Ast. Rep.*, 53(5), 436  
 Wheatley, P. J., Mauche, C. W., & Mattei, J. A., 2003, *MNRAS*, 345, 49